Universal bound and scattering properties for two dipoles

Yujun Wang and Chris H. Greene
Department of Physics and JILA, University of Colorado, Boulder, Colorado 80309-0440, USA
(Received 21 December 2011; published 10 February 2012)

The bound state and low-energy scattering properties of two oriented dipoles are investigated for both bosonic and fermionic symmetries. Interestingly, a universal scaling emerges for the expectation value of the angular momentum for deeply bound two-dipole states. This scaling traces to the pendulum motion of two dipoles in the strong dipole regime. The low-energy scattering phase shifts of two dipoles also show universal behavior. These universal observations make connections to the scaling laws reported by Wang *et al*. [Phys. Rev. Lett. **106**, 233201 (2011); **107**, 233201 (2011)] for three dipoles.

DOI: 10.1103/PhysRevA.85.022704 PACS number(s): 34.50.−s

I. INTRODUCTION

The recent experimental realization of ultracold polar molecules [1] has attracted tremendous attention because of their potential future applications in studies of astrophysics, condensed matter physics, quantum computing, and ultracold chemistry [2,3]. It also provides great opportunity for studies of few-body physics due to the long-range, anisotropic nature of the molecular interactions in the presence of an external electric field. For polar molecules that have exothermal reaction paths [4], the high short-range reaction probability leads to large ultracold reaction rates that have been observed in experiments and have also been explained by a universal theory [5–11]. Novel phenomena involving polar molecules [2,3] are in particular expected from the long-range interactions. When the molecules are nonreactive, rich resonant features that are tunable via an external field have been predicted in the scattering of two molecules in different geometries [12–21]. Interestingly, these resonances are formed with different mechanisms [15] and therefore occur in an irregular order.

Whereas two-dipole physics has proven to be surprisingly complicated, the three-dipole physics near two-dipole resonances manifests simple universal behavior for both bosonic [22] and fermionic [23] dipoles. This is quite counterintuitive considering that a three-body problem is generally more complicated when compared to a two-body problem. Moreover, in contrast to the previously known three-body systems where nonuniversal short-range physics is important even at unitarity [24], a system with three dipoles at unitarity can be universally defined by two-dipole physics that is characterized by the dipole length d_ℓ defined as

$$d_\ell = m d_m^2 / 2\hbar^2, \tag{1}$$

where d_m is the magnitude of the electric dipole moment induced by an external electric field [18] and m is the mass of a dipole. A close relationship between two- and three-dipole problems is also manifested in the effective repulsion between a dipole and a deeply bound dipolar dimer that has been identified in Refs. [22,23].

In the present work we study universal two-dipole physics that can be relevant to the three-dipole physics mentioned above. In particular, the properties of deeply and weakly bound dipolar states as well as the behavior of the low-energy scattering phase shifts are discussed for both bosonic and fermionic dipoles. It will be shown that when the dipolar interaction is off-resonant, the binding energy of two dipoles scales like $1/md_\ell^2$, and the size of the corresponding state grows linearly with d_ℓ. For deeply bound states, the expectation value $\langle \hat{L}^2 \rangle$ shows universal $\sqrt{d_\ell}$ scaling, where $\hat{L}$ is the angular momentum operator. As will be shown, this scaling traces to the pendulum motion of two dipoles in a strong external field. Finally, universal scaling behavior will be shown for both the real part and and the imaginary part of the phase shifts that characterize elastic scattering and the scattering into different angular momentum channels, respectively.

This paper is organized as follows. Section II introduces our model and method for solving the two-dipole problem. Section III discusses the bound-state properties of the dipoles, and Sec. IV discusses the scattering properties. Finally, we summarize our results in Sec. V. Atomic units are used throughout this work.

II. THEORY

To a good approximation at long range the dipolar molecules in an external field can be treated as point dipoles fully oriented along the field direction. The Schrödinger equation for two dipoles in spherical coordinates is given by

$$\left[-\frac{1}{m}\frac{1}{r}\frac{d^2}{dr^2} r + \frac{\hat{L}^2}{mr^2} + V_{\rm dd} \right] \psi = E\psi, \tag{2}$$

where $V_{\rm dd}$ is the interaction between two dipoles that are oriented to the direction of the external field $\hat{z}$:

$$V_{\rm dd} = \frac{2d_\ell}{m} \frac{1 - 3(\hat{z}\cdot\hat{r})^2}{r^3} f(r). \tag{3}$$

The function $f(r) = \tanh(r/r_0)^{18}$ cuts off the dipolar interaction around the short-range length scale r_0, which avoids an unphysical collapse of the system in the case of the $-1/r^3$ singularity at the origin. For alkali-metal dipolar molecules used in ultracold experiments, r_0 is determined by the distance where the short-range van der Waals interaction ($\sim 1/r^6$) starts dominating over the dipolar interaction. The ratio d_ℓ/r_0 that defines the dipole regime ($d_\ell/r_0 \gg 1$) and the van der Waals regime ($d_\ell/r_0 \ll 1$) can change from 0 at zero external electric field to more than 10^3 for fully polarized dipolar molecules [11]

In the presence of anisotropic interactions, an appropriate angular representation can provide deep physical insight and quick numerical convergence. An expansion of angular motion using spherical harmonics that are defined on a numerical

grid has been used in Ref. [25] to efficiently solve scattering with anisotropic interactions, including dipoles that are not aligned. In our study, a simple partial wave expansion (diabatic representation) is adequate for our study of dipolar scattering while the adiabatic representation is better suited for the study of deeply bound dipolar states.

A. Diabatic representation

To solve Eq. (2), it is natural to expand ψ in the basis of angular momentum eigenstates $|lm_l\rangle$ as

$$\psi^{m_l} = \frac{1}{r}\sum_{l'} F_{l'}^{m_l}(r)|l'm_l\rangle, \tag{4}$$

where different m_l decouple when the quantization axis is along the direction of the external field. For large r, different $|lm_l\rangle$ states decouple and physically serve as scattering channels for two dipoles. In this basis, Eq. (2) reduces to a set of coupled equations:

$$\left[-\frac{1}{m}\frac{d^2}{dr^2} + \frac{l(l+1)}{mr^2}\right]F_l^{m_l}(r) + \frac{d_\ell}{mr^3}\sum_{l'} D_3(m_l;l,l')F_{l'}^{m_l}(r) = E F_l^{m_l}(r), \tag{5}$$

where the coupling coefficients $D_3(m_l;l,l')$ are expressed in terms of 3-j symbols:

$$D_3(m_l;l,l') = (-1)^{m_l+1}4\sqrt{(2l+1)(2l'+1)}\begin{pmatrix} l & 2 & l' \\ 0 & 0 & 0 \end{pmatrix}\begin{pmatrix} l & 2 & l' \\ -m_l & 0 & m_l \end{pmatrix}. \tag{6}$$

Note that l and l' are coupled only when $|l'-l| \leqslant 2$ and specifically when $|l'-l| = 2$ for indistinguishable dipoles that are considered in the present work.

B. Adiabatic representation

Another way to solve Eq. (2) is to use the adiabatic representation, as has been implemented in Refs. [15–18]. It has been shown [15–18] that the adiabatic representation gives better characterization of the various dipolar resonances [15,17,18], presumably because the adiabatic channels are less coupled than the angular momentum basis at small distances. At large distances the adiabatic basis reduces to the angular momentum basis, so both representations will give the same scattering matrix. Although these two representations are physically equivalent, we would like to compare their efficiencies and use the one that is the most convenient for our study that involves both analytical and numerical work.

In the adiabatic representation, the two-dipole wave function is expanded in the adiabatic basis ϕ_ν as

$$\psi^{m_l} = \frac{1}{r}\sum_{\nu'} \tilde{F}_{\nu'}^{m_l}(r)\phi_{\nu'}^{m_l}(r;\Omega), \tag{7}$$

where Ω represents the polar angle θ and the azimuthal angle φ, and ν and ν' are the adiabatic channel indices. The adiabatic channel functions $\phi_{\nu'}^{m_l}$ are obtained by solving the adiabatic equation

$$\left(\frac{\hat{L}^2}{mr^2} + V_{\rm dd}\right)\phi_\nu^{m_l}(r;\Omega) = U_\nu(r)\phi_\nu^{m_l}(r;\Omega). \tag{8}$$

Upon substitution of the adiabatic expansion, Eqs. (7)–(2) also takes a multichannel form:

$$\left[-\frac{1}{m}\frac{d^2}{dr^2} + U_\nu(r)\right]\tilde{F}_\nu^{m_l}(r) + \frac{1}{m}\sum_{\nu'}\left[P_{\nu,\nu'}\frac{d}{dr} + \frac{d}{dr}P_{\nu,\nu'}\right]\tilde{F}_{\nu'}^{m_l}(r) + \frac{1}{m}\sum_{\nu'} Q_{\nu,\nu'}\tilde{F}_{\nu'}^{m_l}(r) = E\tilde{F}_\nu^{m_l}(r), \tag{9}$$

but is now characterized by the nonadiabatic couplings $P_{\nu,\nu'}(r)$ and $Q_{\nu,\nu'}(r)$, defined as

$$P_{\nu,\nu'}(r) = \left\langle \langle\phi_\nu|\frac{d}{dr}|\phi_{\nu'}\rangle \right\rangle, \quad Q_{\nu,\nu'}(r) = \left\langle\left\langle \frac{d}{dr}\phi_\nu \middle| \frac{d}{dr}\phi_{\nu'}\right\rangle\right\rangle. \tag{10}$$

The double brackets in the above definition indicate integration over the angles Ω.

In the asymptotic region ($r \gg d_\ell$), the adiabatic channel functions ϕ_ν can be calculated perturbatively from $|lm_l\rangle$, which allows us to analytically derive the asymptotic form of the nonadiabatic couplings. To calculate the leading order of the nonadiabatic couplings $P_{\nu,\nu'}$ for channels ν and ν' that asymptotically approach the diabatic channels (l_ν,m_l) and $(l_{\nu'},m_l)$, respectively, the following expansion of the channels functions is required:

$$\phi_\nu = \sum_{n=\nu}^{\nu'} \eta_n^\nu |l_n m_l\rangle. \tag{11}$$

The expansion coefficients η_n^ν are obtained by $|n-\nu|$th order perturbation theory:

$$\eta_n^\nu = C_n^\nu (d_\ell/r)^{|n-\nu|}, \tag{12}$$

where

$$C_n^\nu = \prod_{k=0}^{n-\nu\mp1}\frac{D_3(m_l;l_\nu+2k,l_\nu+2k\pm2)}{l_\nu(l_\nu+1)-(l_\nu+2k\pm2)(l_\nu+2k\pm2+1)}, \quad C_\nu^\nu = 1. \tag{13}$$

In the above expression the upper sign is taken when $n > \nu$, and the lower signis taken when $n < \nu$. The leading order term in the asymptotic expansion of $P_{\nu,\nu'}$ is then calculated as

$$P_{\nu,\nu'} \simeq -\frac{d_\ell^{|\nu-\nu'|}}{r^{|\nu-\nu'|+1}}\sum_{n=\nu}^{\nu'\mp1}|\nu'-n|C_n^\nu C_n^{\nu'}. \tag{14}$$

Here the upper and lower signs are taken for $\nu' > \nu$ and $\nu' < \nu$, respectively.

Deriving the leading order expression for $Q_{\nu,\nu'}$ requires an expansion of ϕ_ν with two more terms:

$$\phi_\nu = \sum_{n=\nu\mp1}^{\nu'\pm1}\eta_n^\nu|l_n m_l\rangle, \tag{15}$$

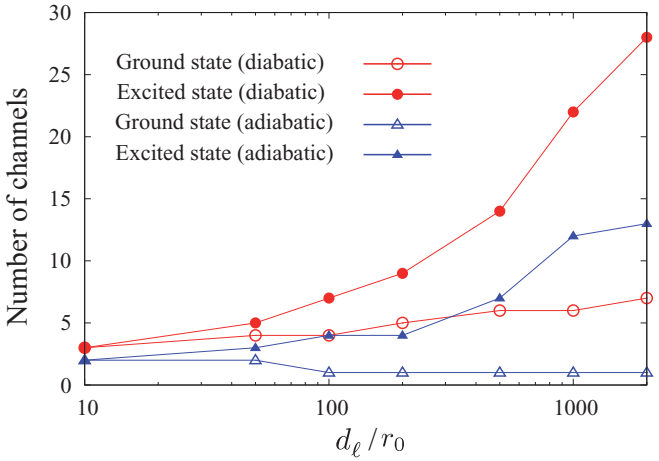

FIG. 1. (Color online) Number of channels required for converging the dipolar bound states within 1% in the diabatic (spherical harmonic) and the adiabatic representations.

where the upper and lower signs are taken for $\nu' > \nu$ and $\nu' < \nu$, respectively. This expansion gives, for $\nu' = \nu$,

$$Q_{\nu,\nu} \simeq \frac{d_\ell^2}{r^4}\left[\left(C^{\nu}_{\nu-1}\right)^2 + \left(C^{\nu}_{\nu+1}\right)^2\right]; \tag{16}$$

for $|\nu' - \nu| = 1$,

$$Q_{\nu,\nu'} \simeq \frac{d_\ell^3}{r^5}\left\{2\left(C^{\nu}_{\nu\pm1}C^{\nu'}_{\nu'\pm2} + C^{\nu}_{\nu\mp2}C^{\nu'}_{\nu'\mp1}\right) - \left[\left(C^{\nu}_{\nu\pm1}\right)^2 C^{\nu'}_{\nu'\pm1} + \left(C^{\nu'}_{\nu'\mp1}\right)^2 C^{\nu}_{\nu\mp1}\right]\right\}; \tag{17}$$

and for $|\nu' - \nu| \geqslant 2$,

$$Q_{\nu,\nu'} \simeq \frac{d_\ell^{|\nu-\nu'|+2}}{r^{|\nu-\nu'|+4}} \sum_{n=\nu\pm1}^{\nu'\mp1} |(n-\nu)(n-\nu')| C^{\nu}_{n\pm1}C^{\nu'}_{n\mp1}. \tag{18}$$

In all the above expressions for $Q_{\nu,\nu'}$, the upper and lower signs are taken for $\nu' > \nu$ and $\nu' < \nu$, respectively. All the above asymptotic behavior for the nonadiabatic couplings has been verified by our numerical calculations.

C. Comparison of diabatic and adiabatic representations

In the following we give a brief comparison of the diabatic and adiabatic representations concerning their convergence with the number of channels. Figure 1 shows the convergence pattern for the energies of the ground state and the highest excited state with respect to the number of channels as d_ℓ increases. Generally, the adiabatic representation converges more quickly, and particularly for deeply lying states it gives better convergence for larger d_ℓ. For high-lying states more channels are required in order to reach convergence for larger d_ℓ in both representations.

The quick convergence of the adiabatic representation for the deeply-bound dipolar states makes it most advantageous in our analytical study of these states in Sec. III A. For studies of the weakly bound states or scattering, however, the adiabatic potentials and nonadiabatic couplings for high-lying channels at small distances ($r \lesssim d_\ell$) cannot be analytically determined and require numerical diagonalization. Therefore even though the adiabatic representation gives faster convergence it does not provide significantly better performance, and we will use the diabatic representation since it can be more easily generated in calculations of weakly bound states and scattering.

III. BOUND STATE PROPERTIES

A. Deeply bound states

In the presence of a strong external field, dipoles in a deeply bound state tend to align themselves in the linear configuration where the dipolar potential, Eq. (3), is angularly minimal. For small polar angles θ, Eq. (3) can be approximated by

$$V_{\rm dd} \approx \frac{2d_\ell}{m}\frac{-2+3\theta^2}{r^3}, \tag{19}$$

which corresponds to a harmonic potential in the θ direction with a trapping frequency of $\omega = \sqrt{24 d_\ell/m^2 r}$ and a zero-point angle given by

$$\theta_0 = \sqrt{\frac{2}{m\omega}} = 6^{-1/4}\left(\frac{d_\ell}{r}\right)^{-1/4}. \tag{20}$$

As d_ℓ increases, two dipoles in a deeply bound state become more angularly localized and undergo pendulum motion within an angle roughly determined by θ_0. The expectation value of the angular momentum $\langle \hat{L}^2 \rangle$ is therefore expected to grow with d_ℓ.

In view of the connection between $\langle \hat{L}^2 \rangle$ and the barrier in the collision of a dipole and a dipolar dimer [22,23], the following studies the scaling of $\langle \hat{L}^2 \rangle$ with d_ℓ. The adiabatic approximation of the two-dipole solution, Eq. (7), takes the following form:

$$\psi^{m_l}_{n,\nu} = \frac{1}{r}\tilde{F}^{m_l}_{n,\nu}(r)\phi^{m_l}_{\nu}(r;\Omega), \tag{21}$$

where n indicates the approximate quantum number for the radial motion. The angular wave function $\phi^{m_l}_{\nu}$ for the harmonic potential, Eq. (19), can be directly written down in terms of the associated Laguerre polynomials $L^{\alpha}_{n}(x)$:

$$\phi^{m_l}_{\nu} = \sqrt{\frac{2}{\theta_0^2}\frac{\Gamma(\nu+1)}{\Gamma(\nu+|m_l|+1)}}\left(\frac{\theta}{\theta_0}\right)^{|m_l|} L^{|m_l|}_{\nu}\left(\frac{\theta^2}{\theta_0^2}\right) \times e^{-\frac{1}{2}\frac{\theta^2}{\theta_0^2}}\frac{1}{\sqrt{2\pi}}e^{im_l\varphi}. \tag{22}$$

By using the approximate angular momentum operator for $\theta \ll 1$:

$$\hat{L}^2 \approx -\frac{1}{\theta}\frac{\partial}{\partial\theta}\theta\frac{\partial}{\partial\theta} - \frac{1}{\theta^2}\frac{\partial^2}{\partial\varphi^2}, \tag{23}$$

$\langle \hat{L}^2 \rangle$ can be determined as

$$\langle \hat{L}^2 \rangle \approx \sqrt{d_\ell}(2\nu+|m_l|+1)\sqrt{6}\left\langle \frac{\tilde{F}^{m_l}_{n,\nu}}{r}\middle|\frac{1}{\sqrt{r}}\middle|\frac{\tilde{F}^{m_l}_{n,\nu}}{r}\right\rangle. \tag{24}$$

Since for deeply bound states the radial wave fuction $\tilde{F}^{m_l}_{n,\nu}$ is localized around $r \lesssim r_0$, the radial integral should scale with $1/\sqrt{r_0}$ and $\langle \hat{L}^2 \rangle$ is expected to obey the following scaling

$$\langle \hat{L}^2 \rangle \propto \sqrt{\frac{d_\ell}{r_0}}(2\nu + |m_l| + 1). \tag{25}$$

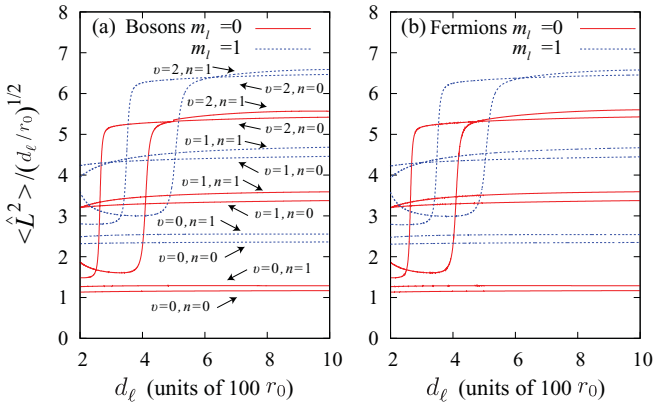

FIG. 2. (Color online) The scaled angular momentum expectation value $\langle \hat{L}^2 \rangle / (d_\ell / r_0)^{1/2}$ for bosonic dipoles (a) and fermionic dipoles (b).

It is interesting to note that this scaling is independent of the identical particle symmetry. This can be simply understood from the angular localization of a pendulum wave function that makes the exchange effect negligible.

Figure 2 shows the angular momentum expectation value $\langle \hat{L}^2 \rangle$ calculated numerically. The quick changes in $\langle \hat{L}^2 \rangle$ at small d_ℓ are related to the transition of the dipolar states from a single angular momentum character to a pendulum character. The angular and radial excitations for the corresponding dipolar states can be seen from the wave functions shown in Fig. 3. The equally spaced $\langle \hat{L}^2 \rangle$ from numerical calculations suggests the validity of the approximated scaling in Eq. (25). The radial excitations n introduce splittings on top of the

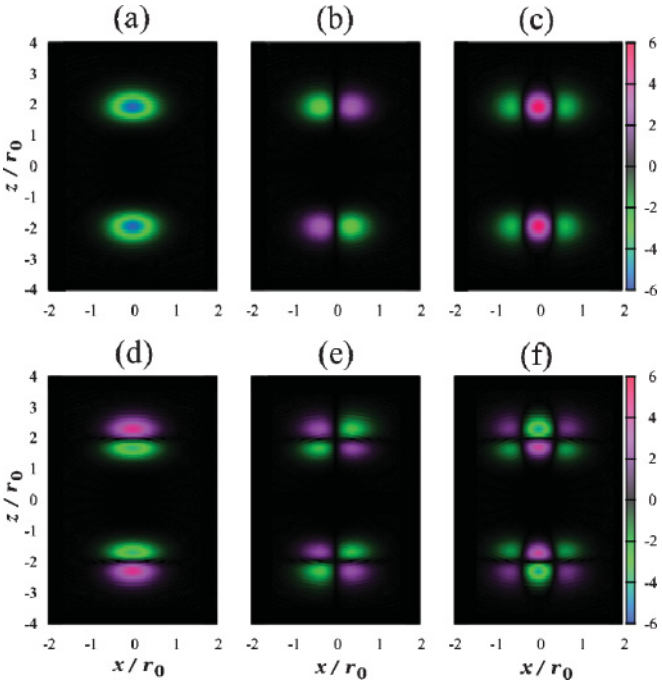

FIG. 3. (Color online) The cuts of the deeply bound two-dipole wave function along the x-z plane for bosons. Different angular and radial excitations $(|m_l|, v, n)$ are shown: (a) (0,0,0), (b) (1,0,0), (c) (0,1,0), (d) (0,0,1), (e) (1,0,1), and (f) (0,1,1). The dipole length $d_\ell = 600 r_0$ for all these wave functions.

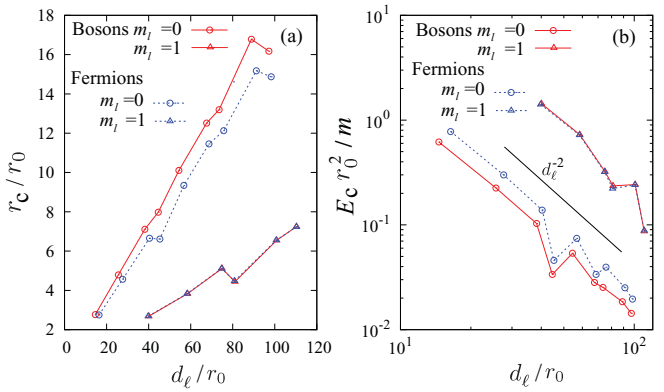

FIG. 4. (Color online) The characteristic size r_c (a) and the characteristic energy $|E_c|$ (see text) (b) for both bosonic and fermionic dipoles with $|m_l| = 0$ and 1. The irregular jumps come from the avoided crossings between states with different angular momentum character.

scaling given by Eq. (25), but such splittings become finer with a sharper short-range cutoff function $f(r)$ as both expected from Eq. (24) and verified by our numerical calculations.

B. Weakly bound states

For weakly bound states, we first discuss the properties of such states away from a dipole-dipole resonance. These properties are important in determining the scaling laws for three-dipole recombination [22] and possibly also for the vibrational relaxation of a weakly bound dipolar dimer in an off-resonant situation. To this end, we introduce the characteristic size r_c and the characteristic energy E_c for the weakly bound dipolar states as the expectation value of r and the energy, respectively, for the state that is right below a zero-energy bound state.

Figure 4 shows numerically calculated r_c and E_c as d_ℓ increases. In all cases it is shown that $r_c \propto d_\ell$ and $E_c \propto 1/m d_\ell^2$. These scalings contrast interestingly with the deeply bound

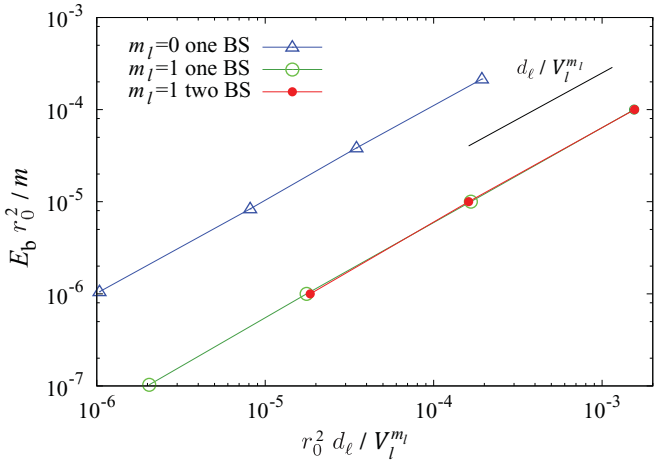

FIG. 5. (Color online) The scaling behavior of the binding energy E_b with d_ℓ and $V_l^{m_l}$ near p-wave resonances for fermionic dipoles. The dipole length d_ℓ is tuned to have one or two bound states (BS) for $m_l = 0$ and $m_l = 1$.

states, where the sizes of the states shrink to r_0 and the energies grow deeper linearly with d_ℓ.

Near a dipole-dipole resonance where a zero-energy bound state is formed, the binding energy of a weakly bound state is closely related to the low-energy expansion of the scattering phase shift. In the presence of the s-wave contribution ($m_l = 0$ for bosons) the binding energy E_b can be written in terms of the s-wave scattering length $a_{l=0}^{m_l}$ as $E_b \approx 1/m(a_{l=0}^{m_l})^2$ by finding the pole in the scattering amplitude [26]. When s-wave contribution is absent, searching for a pole in the scattering amplitude is not straightforward due to an anomalous low-energy expansion of the phase shifts [see Eq. (30)]. Nevertheless, near a p-wave resonance for fermions we have numerically identified that $E_b \propto d_\ell / V_{l=1}^{m_l}$, where the scattering volume $V_l^{m_l}$ diverges near a p-wave resonance. As shown in Fig. 5, the proportionality constant in the scaling of E_b depends on m_l but is independent of the short-range interaction details as the number of bound states changes.

IV. LOW-ENERGY SCATTERING PROPERTIES

In previous studies of two-dipole elastic scattering [12–21], the behavior of the scattering cross sections has been studied quite extensively. Our goal here, however, is to study the two-dipole scattering by examining the low-energy expansion of the phase shifts. Of particular interest are the phase shifts from the lowest partial wave, which is the most sensitive to the dipole-dipole resonances at zero energy.

In the present case where the angular momentum is not conserved, we define the phase shifts $\delta_l^{m_l}$ from the diagonal scattering matrix elements $S_{l,l}^{m_l}$:

$$\delta_l^{m_l} = \ln\left(S_{l,l}^{m_l}\right)/2i. \tag{26}$$

In the presence of couplings between different partial waves, $\delta_l^{m_l}$ acquires an imaginary part that characterizes off-diagonal scattering amplitudes. The real part of $\delta_l^{m_l}$ controls the elastic scattering. While dipole-dipole scattering is multichannel, some insights into the low-energy expansion for $\mathrm{Re}[\delta_l^{m_l}(k)]$ can be gained from the single-channel scattering with a $1/r^3$ potential [27–29]: $\mathrm{Re}[\delta_l^{m_l}(k)] \sim -a_l^{m_l}k$, where $k = \sqrt{mE}$ is the scattering wave number.

The effective range expansion for short-range potentials [30,31] has the following low-energy expansion of the phase shift:

$$\delta_l(k) = -ak - Vk^3 + O(k^5), \tag{27}$$

where the power of k increases by 2 for consecutive terms. For dipolar scattering, however, our numerical study shows that the phase shifts are in expansions with increments of k for all partial waves:

$$\mathrm{Re}\left[\delta_l^{m_l}(k)\right] = -a_l^{m_l}k - b_l^{m_l}k^2 - V_l^{m_l}k^3 + O(k^4). \tag{28}$$

Our discussion here is restricted up to the term that starts showing nonuniversal behavior. As has been shown in previous works [12–18], the scattering length $a_l^{m_l}$ shows nonuniversal resonant behavior for $l = 0$. We have further verified that in this case the resonant behavior persists in all higher terms. For fermionic dipoles, our numerical study shows nonuniversal resonant behavior starting from $V_{l=1}^{m_l}$, while $b_{l=1}^{m_l}$ remains universal. Nonuniversal resonant behavior is therefore expected to start from the term of k^{2l_0+1} for only $l = l_0$, where l_0 is the lowest partial wave allowed for a given symmetry. For the terms lower than k^{2l_0+1} the coefficients are expected to be universally determined by d_ℓ.

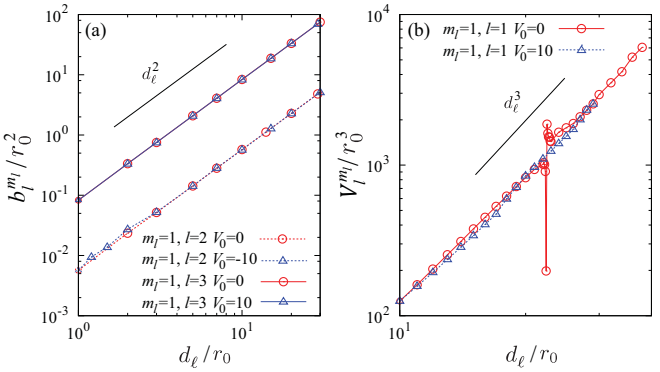

FIG. 6. (Color online) (a) The d_ℓ dependence of the coefficient $b_l^{m_l}$ in the low-energy expansion of $\mathrm{Re}[\delta_l^{m_l}(k)]$. (b) The d_ℓ dependence of the scattering volume $V_l^{m_l}$.

For $l > 0$, Bohn *et al.* [16] have analytically derived a universal expression for the T matrix to the leading order in k; the results can be readily used to give the following expression for $a_l^{m_l}$,

$$a_l^{m_l} = d_\ell \frac{D_3(m_l;l,l)}{2l(l+1)}. \tag{29}$$

Next we study the scaling behavior of $b_l^{m_l}$ and the scattering volume $V_l^{m_l}$ by numerical calculations. The universality is tested by adding an isotropic short-range interaction $V_{\mathrm{iso}} = V_0\mathrm{sech}^2(r/r_0)$. Figure 6(a) shows the d_ℓ dependence of a few $b_l^{m_l}$ with different V_0. It is clearly seen that $b_l^{m_l}$ follows a d_ℓ^2 scaling behavior that is independent of V_0. An exception for this universal behavior is $b_{l=0}^{m_l=0}$, where the nonuniversal resonant behavior already begins in the lower term $a_{l=0}^{m_l=0}$. Nevertheless, $b_{l=0}^{m_l=0}$ is found to follow a universal d_ℓ^2 background scaling with nonuniversal resonant features on top. Table I lists some numerically determined scaling coefficients.

The study of scattering volume is more challenging due to the difficulty to numerically fit Eq. (30) to the third order accurately. Our numerical study shows that the scattering volume $V_l^{|m_l|}$ follows a d_ℓ^3 scaling in general. For $l = 1$, the lowest partial wave allowed for fermionic scattering, nonuniversal resonant features are expected for $V_{l=1}^{|m_l|}$. Nevertheless, a universal d_ℓ^3 background scaling can be identified

TABLE I. The numerically calculated universal scaling for the phase-shift expansion coefficient $b_l^{m_l}$ for a few symmetries.

m_l	l	$b_l^{m_l}$ (units of d_ℓ^2)
0	1	-2.60×10^{-1}
0	2	2.56×10^{-2}
0	3	2.30×10^{-3}
1	1	-8.32×10^{-2}
1	2	-5.70×10^{-3}
1	3	1.27×10^{-3}

from Fig. 6(b). The positions of the resonant features clearly depend on the short-range interaction as tuned by V_0, but the background scaling remains unaltered.

Finally we discuss the low-energy expansion for the imaginary part for the phase shift $\mathrm{Im}[\delta_l^{m_l}(k)]$. The following expansion,

$$\mathrm{Im}\left[\delta_l^{m_l}(k)\right] = -c_l^{m_l}k^2 + O(k^3), \tag{30}$$

is found from our numerical calculations, indicating a vanishing imaginary part in the scattering length when $kd_\ell \ll 1$. By using the unitary constraint on the diagonal element of the S matrix to leading order, $c_l^{m_l}$ can be determined as

$$c_l^{m_l} = -\frac{d_\ell^2}{12}\left\{\left[\frac{D_3(m_l;l,l-2)}{l(l+1)}\right]^2 + \left[\frac{D_3(m_l;l,l+2)}{(l+1)(l+2)}\right]^2\right\} \tag{31}$$

for all partial waves.

V. SUMMARY

To summarize, we have studied the universal properties for two dipoles. The long-range, anisotropic dipolar interaction brings rich, universal physics that has key implications for the universal three-dipole physics. This is shown particularly for both the deeply bound and the weakly bound sides of the dipolar spectrum. For the deeply bound dipolar states, the pendulum motion between the dipoles gives rise to a universal growth in the expectation value of the angular momentum, which produces a centrifugal barrier between a dipole and a dipolar dimer [22,23]. For the weakly bound states, general scalings of the binding energy and the size of the states are identified, despite the complicated level crossings for states with different angular momentum characters. Finally, the low-energy scattering phase shifts for two dipoles are predominantly determined by the dipole length, with some nonuniversal ingredients that give rise to resonant features.

ACKNOWLEDGMENTS

This work is supported in part by the AFOSR-MURI and by the National Science Foundation. We thank J. P. D'Incao and J. L. Bohn for stimulating discussions.

[1] K.-K. Ni, S. Ospelkaus, M. H. G. de Miranda, A. Pe'er, B. Neyenhuis, J. J. Zirbel, S. Kotochigova, P. S. Julienne, D. S. Jin, and J. Ye, Science **322**, 231 (2008); S. Ospelkaus, K. K. Ni, G. Quemener, B. Neyenhuis, D. Wang, M. H. G. de Miranda, J. L. Bohn, J. Ye, and D. S. Jin, Phys. Rev. Lett. **104**, 030402 (2010); Johann G. Danzl, Manfred J. Mark, Elmar Haller, Mattias Gustavsson, Russell Hart, Jesus Aldegunde, Jeremy M. Hutson, and Hanns-Christoph Näger, Nat. Phys. **6**, 265 (2010).
[2] M. A. Baranov, Phys. Rep. **464**, 71 (2008).
[3] L. D. Carr, D. DeMille, R. V. Krems, and J. Ye, New J. Phys. **11**, 055049 (2009).
[4] P. S. Zuchowski and J. M. Hutson, Phys. Rev. A **81**, 060703(R) (2010).
[5] Z. Idziaszek and P. S. Julienne, Phys. Rev. Lett. **104**, 113202 (2010).
[6] A. Micheli, Z. Idziaszek, G. Pupillo, M. A. Baranov, P. Zoller, and P. S. Julienne, Phys. Rev. Lett. **105**, 073202 (2010).
[7] Z. Idziaszek, G. Quéméner, J. L. Bohn, and P. S. Julienne, Phys. Rev. A **82**, 020703 (2010).
[8] G. Quéméner and J. L. Bohn, Phys. Rev. A **83**, 012705 (2011).
[9] G. Quéméner and J. L. Bohn, Phys. Rev. A **81**, 060701 (2010).
[10] G. Quéméner and J. L. Bohn, Phys. Rev. A **81**, 022702 (2010).
[11] G. Quéméner, J. L. Bohn, A. Petrov, and S. Kotochigova, Phys. Rev. A **84**, 062703 (2011).
[12] B. Deb and L. You, Phys. Rev. A **64**, 022717 (2001).
[13] C. Ticknor and J. L. Bohn, Phys. Rev. A **72**, 032717 (2005).
[14] C. Ticknor, Phys. Rev. A **76**, 052703 (2007).
[15] K. Kanjilal and D. Blume, Phys. Rev. A **78**, 040703(R) (2008).
[16] J. L. Bohn, M. Cavagero, and C. Ticknor, New J. Phys. **11**, 055039 (2009).
[17] V. Roudnev and M. Cavagnero, Phys. Rev. A **79**, 014701 (2009).
[18] V. Roudnev and M. Cavagnero, J. Phys. B **42**, 044017 (2009).
[19] C. Ticknor, Phys. Rev. A **81**, 042708 (2010).
[20] C. Ticknor, Phys. Rev. A **84**, 032702 (2011).
[21] J. P. D'Incao and C. H. Greene, Phys. Rev. A **83**, 030702 (2011).
[22] Y. Wang, J. P. D'Incao, and C. H. Greene, Phys. Rev. Lett. **106**, 233201 (2011).
[23] Y. Wang, J. P. D'Incao, and C. H. Greene, Phys. Rev. Lett. **107**, 233201 (2011).
[24] E. Braaten and H.-W. Hammer, Phys. Rep. **428**, 259 (2006).
[25] V. S. Melezhik and Chi-Yu Hu, Phys. Rev. Lett. **90**, 083202 (2003).
[26] L. D. Landau and E. M. Lifshitz, *Quantum Mechanics* (*Non-relativistic Theory*), 3rd ed., (Oxford, Butterworth-Heinemann, 2003).
[27] B. Gao, Phys. Rev. A **59**, 2778 (1999).
[28] H. R. Sadeghpour, J. L. Bohn, M. J. Cavagnero, B. D. Esry, I. I. Fabrikant, J. H. Macek, and A. R. P. Rau, J. Phys. B **33**, R93 (2000).
[29] B. Gao, Phys. Rev. A **78**, 012702 (2008).
[30] H. A. Bethe, Phys. Rev. **76**, 38 (1949).
[31] R. G. Newton, *Scattering Theory of Waves and Particles*, 2nd ed. (Springer, New York, 1966).